

# Absolute frequency measurement of rubidium 5S-6P transitions

Conny Glaser,<sup>1,\*</sup> Florian Karlewski,<sup>2</sup> Jens Grimmel,<sup>1</sup> Manuel Kaiser,<sup>1</sup> Andreas Günther,<sup>1</sup> Helge Hattermann,<sup>1</sup> and József Fortágh<sup>1</sup>

<sup>1</sup>*Center for Quantum Science, Physikalisches Institut, Eberhard Karls Universität Tübingen, Auf der Morgenstelle 14, D-72076 Tübingen, Germany*

<sup>2</sup>*HighFinesse GmbH, Wöhrdstraße 4, D-72072 Tübingen, Germany*

We report on measurements on the 5S-6P rubidium transition frequencies for rubidium isotopes with an absolute uncertainty of better than 450 kHz for the  $5S \rightarrow 6P_{1/2}$  transition and 20 kHz for the  $5S \rightarrow 6P_{3/2}$  transition, achieved by saturation absorption spectroscopy. From the results we derive the hyperfine splitting with an accuracy of 460 kHz and 30 kHz, respectively. We also verify the literature values for the isotope shifts as well as magnetic dipole constant and the electric quadrupole constant.

## INTRODUCTION

The advent of optical frequency combs has revolutionized the world of high precision spectroscopy and has enabled measurements of atomic transition frequencies with exceptional accuracy [1–3]. Precise knowledge of these frequencies facilitates better calculations of atomic models and the derivation of more accurate values of physical quantities such as the Lamb shift [4], hyperfine structure constants [5], magnetic dipole or electric quadrupole constant. Furthermore, precise knowledge of these values is desirable to experimentally investigate novel ways of manipulating atomic states, such as the coherent excitation of Rydberg atoms for quantum information processing [6, 7], generation of atomic memories [8] or implementing novel quantum gates [9].

For quantum information purposes rubidium Rydberg atoms are a widely used species. A common way to excite Rubidium atoms from the 5S ground state to Rydberg states with high principal quantum numbers  $n$  is via a three level ladder scheme  $5S \rightarrow 5P \rightarrow nS$  or  $nD$  using a pair of lasers with wavelengths 780 nm and 480 nm. This scheme, however, commonly relies on the generation of 480 nm light by frequency-doubling a 960 nm laser, which limits the available laser power [10].

A promising alternative is the excitation using the 6P state as intermediate state [11, 12]. Due to the five times larger lifetime  $\tau = 121$  ns compared to the 5P state [13], dephasing during the excitation is reduced and the coherence time of this transition is expected to be larger [9, 14]. The commercial availability of 420 nm ECDL lasers renders the Rydberg excitation (ladder) scheme via the 6P intermediate state a viable alternative to the commonly used excitation state via the 5P state. Additionally, the light driving the  $6P \rightarrow nS$  transition at 1016 nm can easily be generated with high power using external cavity diode lasers (ECDL) and allows high Rabi frequencies in the excitation to Rydberg states.

While the transition frequencies for the excitation scheme  $5S \rightarrow 5P \rightarrow nS$ ,  $nD$  are known to 6 kHz accuracy

[15], there has been so far no absolute data available for the transition  $5S \rightarrow 6P \rightarrow nS$ ,  $nD$ , which is however necessary for the implementation of quantum information protocols using this excitation path. Knowing the 6P transition frequencies and the fine and hyperfine structure sub-levels with high accuracy, the transition frequencies from the 6P intermediate state to Rydberg states can then be calculated using the quantum defect theory [10, 16–18]. Measurements of the hyperfine splitting of the  $^{85}\text{Rb}$  and  $^{87}\text{Rb}$  6P levels have been performed before [19, 20], but the most accurate value for the absolute frequencies in literature have uncertainties of 850 MHz (0.0005 nm) [21]. Here, we report on the measurements of the absolute frequencies for this transitions and on measurement schemes to determine the relative frequencies. We have measured the absolute frequencies of the  $5S \rightarrow 6P_{3/2}$  resonance with an uncertainty of  $\leq 20$  kHz and better than 450 kHz for the  $5S \rightarrow 6P_{1/2}$  transition, improving the literature values by five and four orders of magnitude, respectively. In addition to verifying the literature values of the isotope shifts and the magnetic dipole and electric quadrupole constants, we have also determined the hyperfine splittings, depicted in Fig. 1, from the measured transition frequencies, which brings their accuracies to the same respective orders of magnitude, improving the literature values by three and two orders of magnitudes.

## EXPERIMENTAL SETUP

Our experimental setup is a saturation spectroscopy as shown in Fig. 2. The laser source is an ECDL with a linewidth of  $< 400$  kHz as measured by the beating signal between the ECDL laser and the frequency comb. The frequency comb is phase-locked to a solid state 1550 nm laser (I15, NKT) with a linewidth of  $< 100$  Hz. The linewidth of the comb is  $< 2$  kHz, which was measured by beating it to a second 1550 nm laser. The pump and probe beams counter-propagate through the heated rubidium vapor cell (321 K). Polarizing beam splitters ensure crossed linear polarizations to avoid interference effects within the cell. A double-layer magnetic  $\mu$ -metal

\* conny.glaser@uni-tuebingen.de

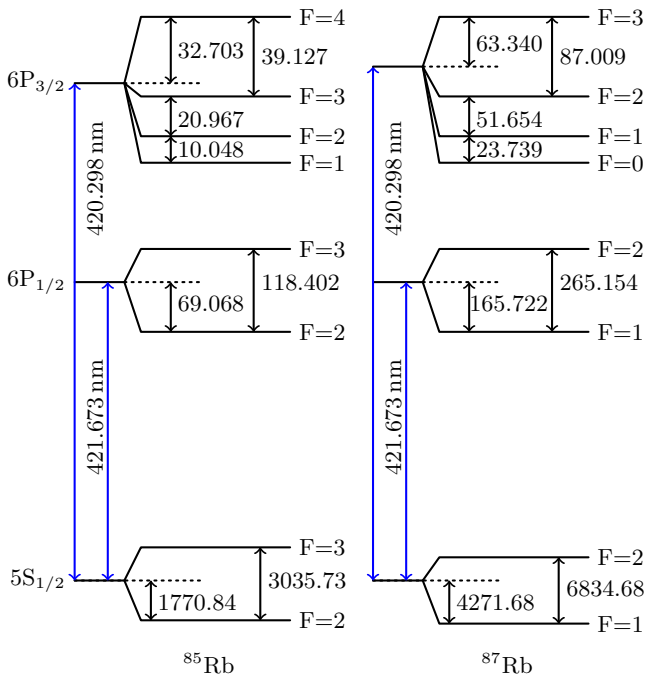


FIG. 1. (Color online) Level scheme and hyperfine splitting (in MHz) for the  $5S_{1/2}$  and  $6P$  manifold of  $^{85}\text{Rb}$  (left) and  $^{87}\text{Rb}$  (right). Drawing not to scale.

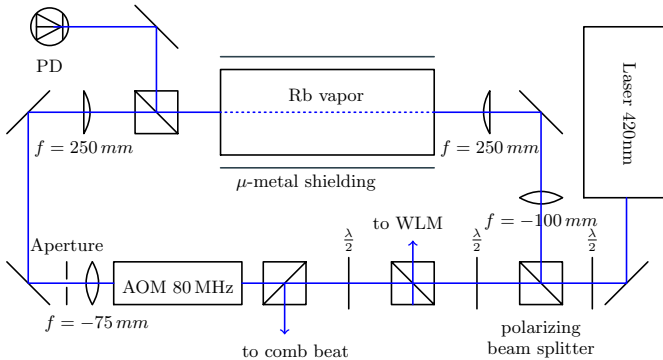


FIG. 2. (Color online) Optical setup for the measurement of the  $5S \rightarrow 6P$  transitions in a rubidium vapor cell. The probe and pump beams are counter propagating in the cell (heated to  $\approx 321\text{ K}$ ). The probe laser intensity is monitored with a photodiode (PD) and the pump beam is chopped with an  $80\text{-MHz}$  acousto-optical modulator (AOM). Both beams originate from an external cavity diode laser, which is either scanned by a wavelength meter (WLM) ( $5S \rightarrow 6P_{1/2}$  transition) or locked to the frequency comb ( $5S \rightarrow 6P_{3/2}$  transition).

shielding leads to a reduction of magnetic fields to less than  $0.03\text{ G}$ , which has been verified with a Gaussmeter (GM07 Gaussmeter, Hirst Magnetic Instruments LTD). The power ratio between probe and pump beams was adjusted in order to optimize the signal-to-noise ratio of the Lamb dips. The optimal ratio was found to be near  $(10:1)$ , using a probe power of  $0.488\text{ mW}$  ( $14.9\text{ mW/cm}^2$ ) and a pump beam power of  $56\text{ }\mu\text{W}$  ( $1.2\text{ mW/cm}^2$ ). The

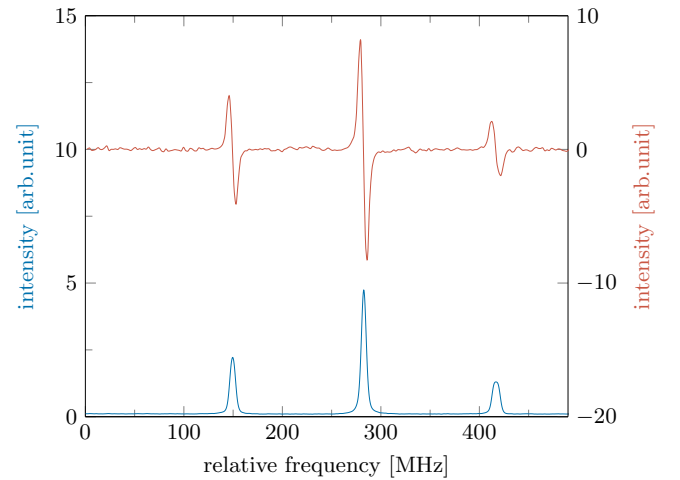


FIG. 3. Doppler free spectrum (blue, color online) and the resulting error signals (red) for the  $^{87}\text{Rb}$   $5S_{1/2}$  ( $F=1$ )  $\rightarrow$   $6P_{1/2}$  transitions.

intensity and the frequency of the pump beam were modulated with a frequency of  $50\text{ kHz}$  using an  $80\text{ MHz}$  acousto-optical modulator (AOM). The probe beam signal from the photodiode was subsequently demodulated at the same frequency using a lock-in Amplifier (HF2LI, Zurich Instruments), which results in a fully Doppler free spectroscopy signal [22], as depicted exemplarily in Fig. 3 (blue line) for the  $^{87}\text{Rb}$   $5S_{1/2}$  ( $F=1$ )  $\rightarrow$   $6P_{1/2}$  ( $F'=1$ ) transitions. Since the AOM shifts the pump beam by  $80\text{ MHz}$  the measured Lamb dips and cross-overs are red-shifted by  $-40\text{ MHz}$ . This offset has been corrected in the final data analysis.

The relative frequencies between the  $5S \rightarrow 6P_{1/2}$  transitions were measured by scanning the laser with a wavemeter and simultaneously recording the wavelength of the laser.

Additionally, we can impose  $3\text{ MHz}$  sidebands by frequency modulation (FM) of the laser diode current. After appropriate demodulation, this leads to a Pound-Drever-Hall-like (PDH) error signal, which can be used to stabilize the laser onto the transition resonance frequency [23]. Fig. 3 shows an exemplary spectrum acquired by the Lock-in amplifier (blue) and the FM error signals (red) for the  $^{87}\text{Rb}$   $5S_{1/2}$  ( $F=1$ )  $\rightarrow$   $6P_{1/2}$  transitions.

We can control the frequency of the laser in three ways: The first is to stabilize the laser frequency with the FM error signal to one of the transitions using a digital laser locking module (DigiLock, TOPTICA). Alternatively, the laser frequency can be stabilized and scanned by the wavelength meter, which is calibrated with a laser that is frequency stabilized to the  $5S_{1/2}$  ( $F=2$ )  $\rightarrow$   $5P_{3/2}$  ( $F'=3$ ) transition of  $^{87}\text{Rb}$  ( $780.246\text{ 291 nm}$ ) via an FM spectroscopy. Those methods were used to measure the absolute and the relative frequencies for both transitions. For the third method the beam of the ECDL and the modes of a narrow linewidth frequency comb (TOPTICA) were superimposed and frequency-filtered by a

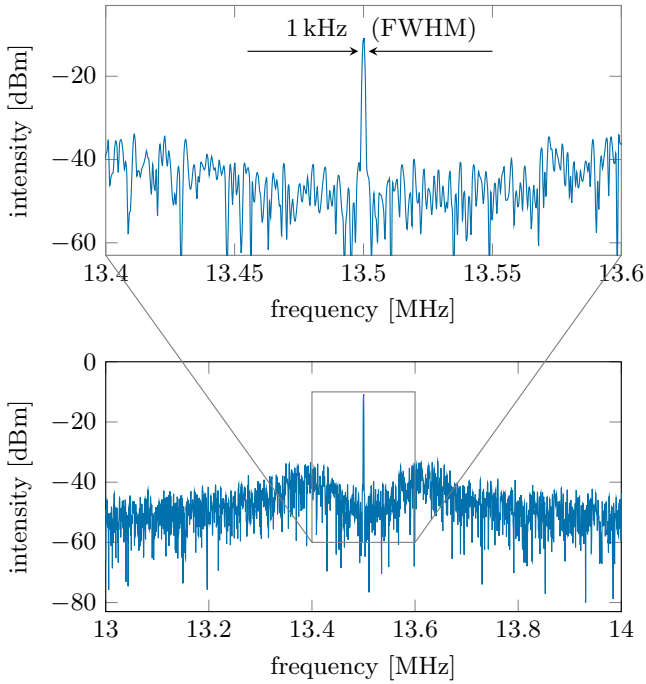


FIG. 4. Typical phase-locked beating signal between a CW laser and a narrow line frequency comb. The upper graph is a zoom into the region of the beating signal, showing a width of  $\approx 1$  kHz.

grating in a beat detection unit (DFC BC and DFC MD, TOPTICA) and monitored on a photodetector with a bandwidth of 50 MHz. The resulting beating signal was acquired with a digital oscilloscope (Picoscope 5442A, Pico Technology). Using the beating signal the 420 nm laser was phase-locked to the frequency comb, using a phase frequency detector (PFD, Toptica) with a filter, that is tunable between 2 and 38 MHz. A typical phase-locked beating signal with a width of  $\approx 1$  kHz can be seen in Fig. 4. The frequency comb is offset-free and its repetition rate  $f_{\text{rep}}=80$  MHz is locked to a GPS-based 10 MHz frequency reference [24] with an accuracy of  $10^{-10}$ . The comb is phase-locked to the 1500 nm laser using a phase frequency detector, which results in comb modes with a linewidth of  $< 5$  kHz, measured by locking the comb to another frequency comb (FC 1500, Menlo). This method to measure the frequencies was only applicable to the  $5S \rightarrow 6P_{3/2}$  transition, since the comb doesn't support the corresponding wavelength to the  $5S \rightarrow 6P_{1/2}$  transition. Fig. 5 shows a typical saturation spectrum for the  $5S \rightarrow 6P_{3/2}$  transition.

#### MEASUREMENT OF THE $5S \rightarrow 6P_{3/2}$ TRANSITIONS

For the measurement of the absolute transition frequencies the ECDL laser was beaten with the frequency comb. The laser was locked to the FM error signal of

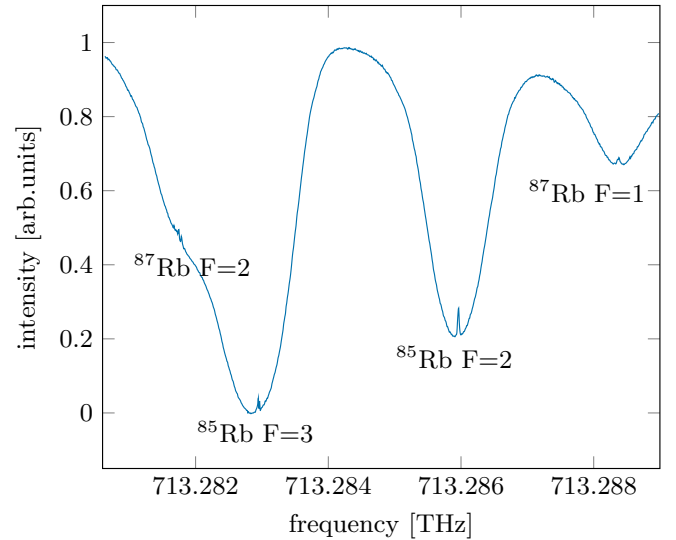


FIG. 5. Saturation spectrum for the  $5S \rightarrow 6P_{3/2}$  transitions for  $^{85}\text{Rb}$  (inner Dips) and  $^{87}\text{Rb}$  (outer dips).

each transition. Simultaneously, the wavemeter recorded the frequency and a digital oscilloscope saved the beat frequency. Knowing these values and the repetition rate of the comb, we were not only able to calculate the absolute frequencies, but also to determine the related comb mode. In order to reduce the statistical error, each measurement was repeated 60 times and subsequently averaged. To characterize the locking accuracy, we locked the 420 nm laser to an arbitrary frequency for 1 h and recorded the beating signal between laser and frequency comb every 15 s. We found that the lock frequency of the laser deviates less than 11.6 kHz/h from its mean value.

The relative frequencies were determined by locking the laser to the frequency comb at a given locking point using the PFD. Starting at the previously measured frequencies and scanning this locking point between 2 and 38 MHz for the corresponding comb mode, the relative frequencies of the  $5S_{1/2} \rightarrow 6P_{3/2}$  transitions can be determined with an accuracy of  $< 1$  kHz resulting from the linewidth of the ECDL laser locked to the frequency comb. Figure 6 shows the resulting spectra from these scans, which have been calibrated using the absolute frequencies from the wavemeter measurement. The gaps in the measured spectra are caused by the locking scheme with the PFD, which can only be tuned between 2 and 38 MHz for each comb mode, since there has to be a frequency difference to the next comb mode. This results in 4 MHz gaps whenever the comb mode has to be changed. All spectra are fitted using a superposition of Pseudo-Voigt profiles, yielding a linewidth of  $\approx 2.7$  MHz (FWHM). The errors arising from the fit routine was calculated separately for each spectrum and were found to be smaller than 20 kHz. The uncertainty in the data for the absolute frequency comprises several known error sources of physical and technical nature. The laser linewidth of the phase-locked

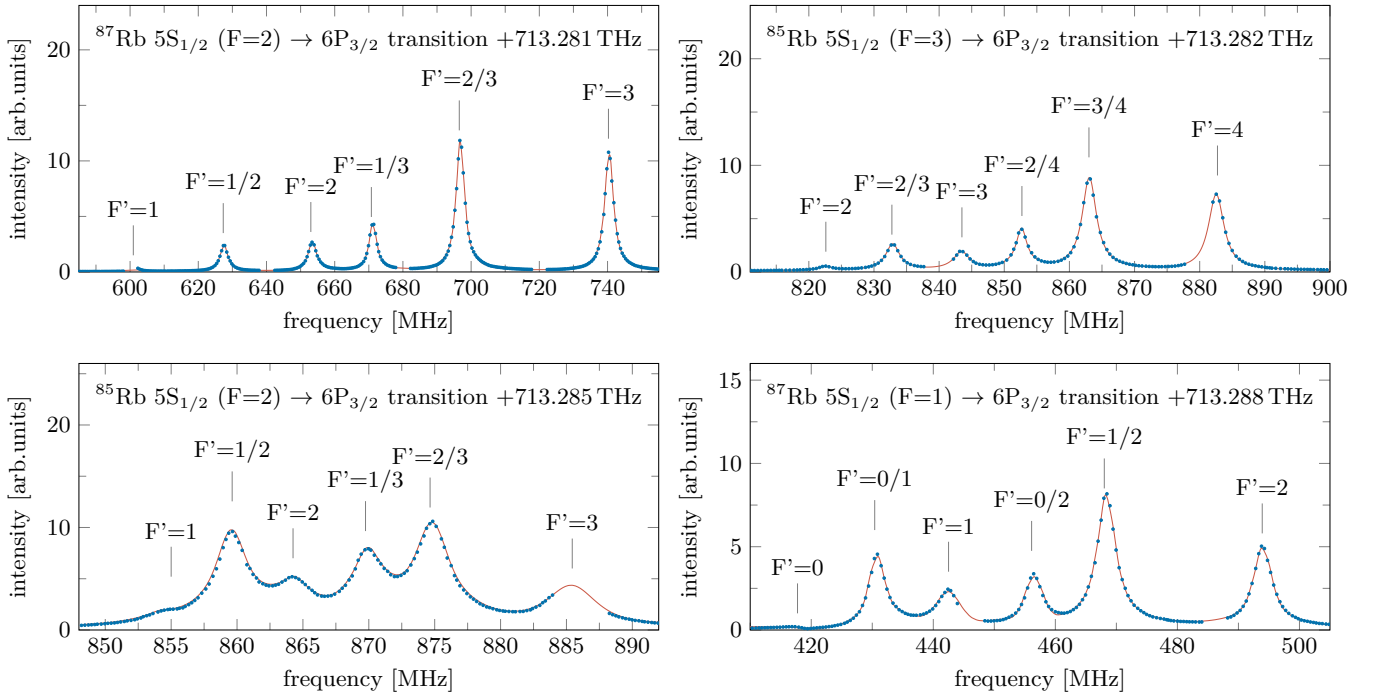


FIG. 6. (Color online) Recorded spectra (blue dots) and fitted superpositions of Pseudo-Voigt functions (red solid line) for the  $5S_{1/2} \rightarrow 6P_{3/2}$  transition. The gaps in the spectra are caused by the PFD locking scheme, which can only be tuned between 2 and 38 MHz for each comb mode, resulting in 4 MHz gaps whenever the comb mode has to be changed.

laser (1 kHz), technical noise and physical deviations cause the fitting error to contribute to the uncertainty of the measured frequency. The overall uncertainty resulting from these effects was determined independently for each measured transition and was found to be  $\leq 20$  kHz. The absolute transition frequencies are summarized in Tab. I.

We have also performed measurements of the absolute transition spectra using the wavemeter to lock the laser. The experimental sequence was as follows: First, the wavelength meter was calibrated as described above. Second, the laser frequency was swept linearly at a rate of 50 MHz/s over a range of 250 MHz while the signal of the lock-in amplifier was recorded. In order to reduce the statistical error, each trace has been measured 100 times and then averaged. The deviations between this measurement and the one including the frequency comb was found to be smaller than 500 kHz.

### MEASUREMENT OF THE $5S \rightarrow 6P_{1/2}$ TRANSITIONS

Since the output of the frequency comb near 420 nm is limited to a range between 418.8 nm and 420.3 nm it was not possible to obtain beating signals for the  $5S_{1/2} \rightarrow 6P_{1/2}$  transition at 421 nm. Therefore, the frequency measurements for this manifold are based on the DigiLock module and wavemeter scans. As determined for the  $5S_{1/2} \rightarrow 6P_{3/2}$  transition, these meth-

ods show deviations of about 500 kHz from each other, so we deem this to be the maximum error. Similarly, as described above, the frequencies were determined by locking the laser to the error signal using the DigiLock. Then the laser was locked to a calibrated wavemeter and swept at a rate of 50 MHz/s over a range of 500 MHz to measure the spectra. Again, each trace was measured 100 times and subsequently averaged, to reduce statistical errors. The resulting spectra are depicted in Fig. 7. We typically measured linewidths (FWHM) of  $\approx 2.8$  MHz, roughly twice as large as expected from the natural linewidth of 1.135 MHz [25]. The positions of the peaks were evaluated by fitting superpositions of Pseudo-Voigt profiles to the spectra. The error due to the fitting routine is on the order of a few kHz and can be neglected compared to the deviations due to the linewidth of the laser. To estimate the error caused by the wavemeter we have characterized its locking accuracy. Therefore we have locked the 420 nm laser to an arbitrary frequency within the output range of the frequency comb for 1 h and recorded the beat signal between laser and a frequency comb mode every 15 s. We found the frequency of the calibrated wavemeter to be normally distributed with a standard deviation of 160 kHz. The total error of the frequencies was calculated to be  $< 450$  kHz, combining the laser linewidth of  $< 400$  kHz and the relative error of the calibrated wavemeter of 160 kHz. The results for the transition frequencies are summarized in Tab. II.

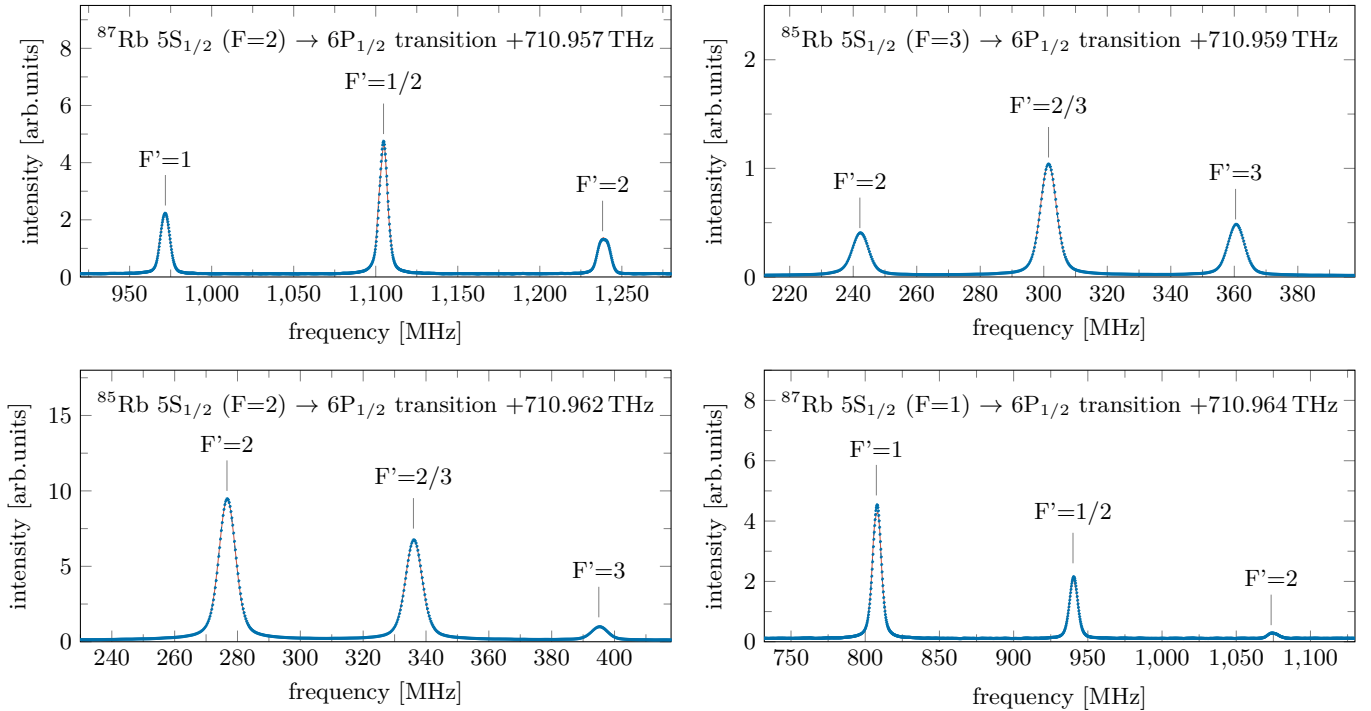


FIG. 7. Recorded spectra (blue dots, color online) and fitted superpositions of Pseudo-Voigt functions (red solid line) for the  $5S_{1/2} \rightarrow 6P_{1/2}$  transitions.

## DISCUSSION

Since pressure broadening is negligible ( $<1$  kHz) and the Zeeman shift caused by the magnetic field is below 10 kHz, the broadening of the natural linewidth discrepancy is assumed to be mostly the consequence of the transversal Doppler effect ( $1 \text{ MHz}/0.12^\circ$ ) and power broadening.

With the measured data we calculated the hyperfine splitting for both transitions. The errors are calculated via propagation of uncertainty based on the transition frequency errors. In Tab. III a comparison between the literature values and the newly determined values is shown.

The total isotope shifts were found to be  $41.935(60)$  MHz for the  $6P_{3/2}$  isotopes and  $41.237(62)$  MHz for the  $6P_{1/2}$  isotopes, which agree well with the literature values [26, 27].

With the determined hyperfine splitting values, the magnetic dipole constant  $A$  and the electric quadrupole constant  $B$  can be calculated for the  $5S \rightarrow 6P$  transitions. The values for each  $^{85}\text{Rb}$  and  $^{87}\text{Rb}$  are listed in Tab. IV and are also in good agreement with the literature data.

## CONCLUSION

In summary, we have performed high precision saturated absorption spectroscopy of  $^{85}\text{Rb}$  and  $^{87}\text{Rb}$  using a diode laser. The laser was stabilized and scanned by a wavelength meter for the  $6P_{1/2}$  transition and locked to a narrow linewidth frequency comb for the  $6P_{3/2}$  transition. This allows for absolute frequency measurements with an uncertainty of  $<20$  kHz for the  $6P_{3/2}$  transition and  $<450$  kHz for the  $6P_{1/2}$  transition. The lower uncertainty in the measurement of the  $5S \rightarrow 6P_{3/2}$  transition results from the laser locking to a narrow line frequency comb, while for the measurement of the  $5S \rightarrow 6P_{1/2}$  transition it is limited by the stability of the wavelength meter. From the measured data we derive hyperfine splitting values with unprecedented accuracy and verified the literature values for the isotope shifts, the magnetic dipole constant and the electric quadrupole constant.

## ACKNOWLEDGEMENTS

This work has been supported by the DFG (SSP 1929 GiRyd and CIT) and BMBF (FKZ: 13N14903). C.G. would like to thank the Evangelische Studienstiftung Vilgigt e.V.

[1] T. Udem, R. Holzwarth, and T. W. Hänsch, *Nature* **416**, 233 (2002).

[2] T. Udem, R. Holzwarth, and T. Hänsch, *The European Physical Journal Special Topics* **172**, 69 (2009).

TABLE I. Measured absolute transition frequencies between the  $5S_{1/2}$  and  $6P_{3/2}$  states of  $^{85}\text{Rb}$  and  $^{87}\text{Rb}$ .

	Transition	Frequency [THz]
$^{87}\text{Rb}$	$F=2 \rightarrow F'=1$	713.281601641(16)
	$F=2 \rightarrow F'=1/2$	713.281627545(16)
	$F=2 \rightarrow F'=2$	713.281653455(16)
	$F=2 \rightarrow F'=1/3$	713.281671206(16)
	$F=2 \rightarrow F'=2/3$	713.281696845(16)
	$F=2 \rightarrow F'=3$	713.281740464(16)
$^{85}\text{Rb}$	$F=3 \rightarrow F'=2$	713.282822529(16)
	$F=3 \rightarrow F'=2/3$	713.282832859(16)
	$F=3 \rightarrow F'=3$	713.282843436(16)
	$F=3 \rightarrow F'=2/4$	713.282852661(16)
	$F=3 \rightarrow F'=3/4$	713.282863062(16)
	$F=3 \rightarrow F'=4$	713.282882547(16)
$^{85}\text{Rb}$	$F=2 \rightarrow F'=1$	713.285854135(18)
	$F=2 \rightarrow F'=1/2$	713.285859657(18)
	$F=2 \rightarrow F'=2$	713.285864366(18)
	$F=2 \rightarrow F'=1/3$	713.285869902(18)
	$F=2 \rightarrow F'=2/3$	713.285874803(18)
	$F=2 \rightarrow F'=3$	713.285885399(18)
$^{87}\text{Rb}$	$F=1 \rightarrow F'=0$	713.288419955(20)
	$F=1 \rightarrow F'=0/1$	713.288430802(20)
	$F=1 \rightarrow F'=1$	713.288442281(20)
	$F=1 \rightarrow F'=0/2$	713.288456485(20)
	$F=1 \rightarrow F'=1/2$	713.288468381(20)
	$F=1 \rightarrow F'=2$	713.288493970(20)

TABLE II. Measured absolute transition frequencies between the  $5S_{1/2}$  and  $6P_{1/2}$  states of  $^{85}\text{Rb}$  and  $^{87}\text{Rb}$ .

	Transition	Frequency [THz]
$^{87}\text{Rb}$	$F=2 \rightarrow F'=1$	710.95797053(45)
	$F=2 \rightarrow F'=1/2$	710.95810465(45)
	$F=2 \rightarrow F'=2$	710.95823892(45)
$^{85}\text{Rb}$	$F=3 \rightarrow F'=2$	710.95924220(45)
	$F=3 \rightarrow F'=2/3$	710.95930147(45)
	$F=3 \rightarrow F'=3$	710.95936053(45)
$^{85}\text{Rb}$	$F=2 \rightarrow F'=2$	710.96227673(45)
	$F=2 \rightarrow F'=2/3$	710.96233612(45)
	$F=2 \rightarrow F'=3$	710.96239520(45)
$^{87}\text{Rb}$	$F=1 \rightarrow F'=1$	710.96480730(45)
	$F=1 \rightarrow F'=1/2$	710.96494083(45)
	$F=1 \rightarrow F'=2$	710.96507276(45)

- [3] S. T. Cundiff and J. Ye, *Rev. Mod. Phys.* **75**, 325 (2003).  
 [4] Y.-J. Huang, Y.-C. Guan, Y.-C. Huang, T.-H. Suen, J.-L. Peng, L.-B. Wang, and J.-T. Shy, *Physical Review A* **97**, 032516 (2018).  
 [5] W.-K. Lee and H. S. Moon, *Phys. Rev. A* **92**, 012501 (2015).  
 [6] M. Saffman, T. G. Walker, and K. Mølmer, *Reviews of Modern Physics* **82**, 2313 (2010).  
 [7] H. Levine, A. Keesling, A. Omran, H. Bernien, S. Schwartz, A. S. Zibrov, M. Endres, M. Greiner, V. Vuletić, and M. D. Lukin, *Physical review letters* **121**, 123603 (2018).  
 [8] K. R. Patton and U. R. Fischer, *Physical review letters* **111**, 240504 (2013).  
 [9] L. Sárkány, J. Fortágh, and D. Petrosyan, *Physical Review A* **92**, 030303(R) (2015).

TABLE III. Hyperfine splitting. The literature values were given without errorbars.

Transition $^{85}\text{Rb}$	Frequency [MHz] [26]	Frequency [MHz]
$6P_{1/2} F=2 - F=3$	117	118.40(46)
$6P_{1/2}$	68.25	69.07(46)
$6P_{3/2} F=1 - F=2$	9	10.048(25)
$6P_{3/2} F=2 - F=3$	21	20.967(25)
$6P_{3/2} F=3 - F=4$	39	39.127(25)
$6P_{3/2}$	32.5	32.703(25)
Transition $^{87}\text{Rb}$	Frequency [MHz] [26]	Frequency [MHz]
$6P_{1/2} F=1 - F=2$	265	265.15(46)
$6P_{1/2}$	165.625	165.72(46)
$6P_{3/2} F=0 - F=1$	24	23.739(26)
$6P_{3/2} F=1 - F=2$	52	51.654(26)
$6P_{3/2} F=2 - F=3$	87	87.009(26)
$6P_{3/2}$	63.331	63.340(26)

TABLE IV. Calculated values for the magnetic dipole constant A and the electric quadrupole constant B.

Transition	Constant	literature [MHz]	this work [MHz]
$^{85}\text{Rb} 5S \rightarrow 6P_{3/2}$	A	8.179(12) [19]	8.174(119)
$^{85}\text{Rb} 5S \rightarrow 6P_{3/2}$	B	8.190(49) [19]	8.113(119)
$^{87}\text{Rb} 5S \rightarrow 6P_{3/2}$	A	27.700(17) [25]	27.716(108)
$^{87}\text{Rb} 5S \rightarrow 6P_{3/2}$	B	3.953(24) [25]	3.983(108)
$^{85}\text{Rb} 5S \rightarrow 6P_{1/2}$	A	39.11(3) [19]	39.47(50)
$^{87}\text{Rb} 5S \rightarrow 6P_{1/2}$	A	132.56(3) [25]	132.83(50)

- [10] M. Mack, F. Karlewski, H. Hattermann, S. Höckh, F. Jessen, D. Cano, and J. Fortágh, *Physical Review A* **83**, 052515 (2011).  
 [11] C. Simonelli, M. Archimi, L. Asteria, D. Capecchi, G. Masella, E. Arimondo, D. Ciampini, and O. Morsch, *Physical Review A* **96**, 043411 (2017).  
 [12] R. Gutiérrez, C. Simonelli, M. Archimi, F. Castellucci, E. Arimondo, D. Ciampini, M. Marcuzzi, I. Lesanovsky, and O. Morsch, *Physical Review A* **96**, 041602(R) (2017).  
 [13] E. Gomez, S. Aubin, L. A. Orozco, and G. D. Sprouse, *J. Opt. Soc. Am. B* **21**, 2058 (2004).  
 [14] L. Sárkány, J. Fortágh, and D. Petrosyan, *Physical Review A* **97**, 032341 (2018).  
 [15] D. A. Steck, "Rubidium 87 d line data," (2001).  
 [16] W. Li, I. Mourachko, M. W. Noel, and T. F. Gallagher, *Phys. Rev. A* **67**, 052502 (2003).  
 [17] J. Han, Y. Jamil, D. V. L. Norum, P. J. Tanner, and T. F. Gallagher, *Phys. Rev. A* **74**, 054502 (2006).  
 [18] K. Afrousheh, P. Bohlouli-Zanjani, J. A. Petrus, and J. D. D. Martin, *Phys. Rev. A* **74**, 062712 (2006).  
 [19] E. Arimondo, M. Inguscio, and P. Violino, *Rev. Mod. Phys.* **49**, 31 (1977).  
 [20] S. Bize, Y. Sortais, M. S. Santos, C. Mandache, A. Clairon, and C. Salomon, *EPL (Europhysics Letters)* **45**, 558 (1999).  
 [21] A. Kramida, Yu. Ralchenko, J. Reader, and NIST ASD Team, NIST Atomic Spectra Database (ver. 5.5.5), [Online]. Available: <https://physics.nist.gov/asd> (2018).  
 [22] J. Ye, S. Swartz, P. Jungner, and J. L. Hall, *Optics letters* **21**, 1280 (1996).

- [23] R. W. P. Drever, J. L. Hall, F. V. Kowalski, J. Hough, G. M. Ford, A. J. Munley, and H. Ward, *Applied Physics B* **31**, 97 (1983).
- [24] T. Puppe, A. Sell, R. Kliese, N. Hoghooghi, A. Zach, and W. Kaenders, *Opt. Lett.* **41**, 1877 (2016).
- [25] M. S. Safronova and U. I. Safronova, *Physical Review A* **83**, 052508 (2011).
- [26] P. Grundevik, M. Gustavsson, A. Rosén, and S. Svanberg, *Zeitschrift für Physik A Atoms and Nuclei* **283**, 127 (1977).
- [27] L. Aldridge, P. L. Gould, and E. E. Eyler, *Physical Review A* **84**, 034501 (2011).